

RESEARCH ARTICLE | MARCH 06 2024

Quantum Drude oscillators coupled with Coulomb potential as an efficient model for bonded and non-covalent interactions in atomic dimers

Matej Ditte ; Matteo Barborini ; Alexandre Tkatchenko  

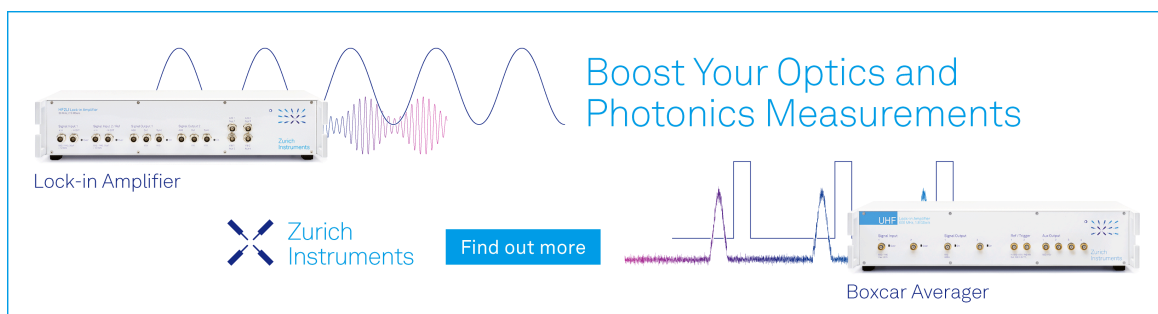


J. Chem. Phys. 160, 094309 (2024)

<https://doi.org/10.1063/5.0196690>



CrossMark



Boost Your Optics and Photonics Measurements

Lock-in Amplifier

Zurich Instruments

Find out more

Boxcar Averager

Quantum Drude oscillators coupled with Coulomb potential as an efficient model for bonded and non-covalent interactions in atomic dimers

Cite as: J. Chem. Phys. 160, 094309 (2024); doi: 10.1063/5.0196690

Submitted: 9 January 2024 • Accepted: 18 February 2024 •

Published Online: 6 March 2024



View Online



Export Citation



CrossMark

Matej Ditte,  Matteo Barborini,  and Alexandre Tkatchenko^{a)} 

AFFILIATIONS

Department of Physics and Materials Science, University of Luxembourg, L-1511 Luxembourg City, Luxembourg

^{a)} Author to whom correspondence should be addressed: alexandre.tkatchenko@uni.lu

ABSTRACT

The quantum Drude oscillator (QDO) model has been widely used as an efficient surrogate to describe the electric response properties of matter as well as long-range interactions in molecules and materials. Most commonly, QDOs are coupled within the dipole approximation so that the Hamiltonian can be exactly diagonalized, which forms the basis for the many-body dispersion method [Phys. Rev. Lett. 108, 236402 (2012)]. The dipole coupling is efficient and allows us to study non-covalent many-body effects in systems with thousands of atoms. However, there are two limitations: (i) the need to regularize the interaction at short distances with empirical damping functions and (ii) the lack of multipolar effects in the coupling potential. In this work, we convincingly address both limitations of the dipole-coupled QDO model by presenting a numerically exact solution of the Coulomb-coupled QDO model by means of quantum Monte Carlo methods. We calculate the potential-energy surfaces of homogeneous QDO dimers, analyzing their properties as a function of the three tunable parameters: frequency, reduced mass, and charge. We study the coupled-QDO model behavior at short distances and show how to parameterize this model to enable an effective description of chemical bonds, such as the covalent bond in the H₂ molecule.

© 2024 Author(s). All article content, except where otherwise noted, is licensed under a Creative Commons Attribution (CC BY) license (<http://creativecommons.org/licenses/by/4.0/>). <https://doi.org/10.1063/5.0196690>

I. INTRODUCTION

The quantum Drude oscillator (QDO) model, first applied by London to describe dispersion interactions between atoms and molecules,¹ was derived from Drude's² classical model of absorption and refraction^{3,4} introduced in 1900. As stated in 1957 by Bade,⁵ “the Drude model provides a means of deriving the second-order dipole–dipole contribution to the London dispersion energy in an especially simple way” and is nowadays at the foundation of many modern van der Waals (vdW) theories^{6–14} used in quantum chemistry and solid-state physics, such as the many-body dispersion (MBD) method.^{11,15,16}

Beyond the original usage of QDOs to model dispersion interactions, this model has been proven to be unusually versatile and extended to capture polarization interactions,^{11,17–19} Pauli repulsion,^{19–21} and optical excitations²² and as a quantum embedding approach for describing molecules in environments.²³

Furthermore, recently, a universal model for the full van der Waals potential between closed-shell atoms has been derived starting from QDOs coupled by multipolar interactions.²⁴ Such versatility of the QDO model raises the question of whether coupled QDOs can be used as a building block for an effective quantum force field with the capacity to describe both short-range (bonded) and long-range (non-bonded) interactions. This work focuses on the fundamental assessment of this question and presents initial evidence for the success of the Coulomb coupled QDO model for constructing efficient and accurate quantum force fields.

Within the QDO model, the response of each atom or molecule²⁵ is represented as an isotropic quantum harmonic oscillator centered at \mathbf{R} with a mass μ and a characteristic frequency ω , described by the following well known Hamiltonian:

$$\hat{h}^D(\mathbf{r}) = -\frac{1}{2\mu}\nabla_{\mathbf{r}}^2 + \frac{1}{2}\mu\omega^2|\mathbf{d}|^2, \quad (1)$$

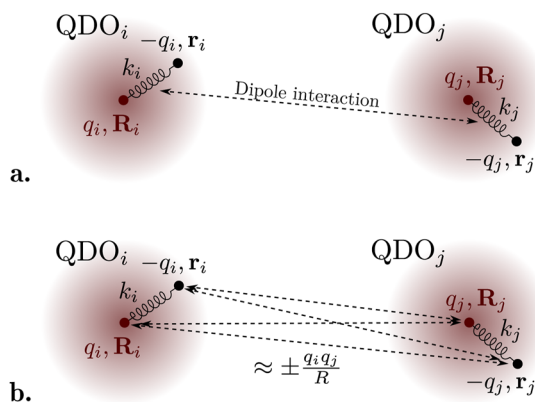


FIG. 1. Schematic representations of the interaction between i th and j th quantum Drude oscillators with force constants $k_i = \mu_i \omega_i^2$ and $k_j = \mu_j \omega_j^2$ coupling via the dipole (a) and full Coulomb (b) potentials.

where $\mathbf{d} = \mathbf{r} - \mathbf{R}$ is the vector distance between the quantum particle, i.e., the drudon, and its center.¹ For a system of N QDOs interacting via the dipole potential, the full Hamiltonian^{5,26,27}

$$\hat{H}^D = \sum_{i=1}^N \hat{h}_i^D(\mathbf{r}_i) + \sum_{j>i=1}^N V_{ij}^D \quad (2)$$

is written as the sum of the Hamiltonians of independent oscillators $\hat{h}_i(\mathbf{r}_i)$ plus the sum of the two-body dipole coupling between the i th and j th oscillators [Fig. 1(a)], written as

$$V_{ij}^D = \frac{q_i q_j}{R_{ij}^3} \left[\mathbf{d}_i \cdot \mathbf{d}_j - \frac{3}{R_{ij}^2} (\mathbf{d}_i \cdot \mathbf{R}_{ij})(\mathbf{d}_j \cdot \mathbf{R}_{ij}) \right], \quad (3)$$

where $\mathbf{R}_{ij} = \mathbf{R}_j - \mathbf{R}_i$ is the vector of the distance between two QDO centers, $R_{ij} = |\mathbf{R}_{ij}|$ is its module, and q_i and q_j are the charges of the dipoles. The parameters of the QDOs are chosen to reproduce the leading order polarizabilities and dispersion coefficients of real matter^{18,20,21} obtained from accurate *ab initio* or experimental data.^{15,20,21,28,29} A considerable advantage of the dipole Hamiltonian in Eq. (2) is that it can be diagonalized,⁵ leading to a simple and efficient way to introduce dispersion interactions,^{30,31} for example, in density-functional theory (DFT) with semilocal exchange–correlation functionals.^{15,32} However, the solution of the dipole Hamiltonian is not defined at all distances⁴ since in the short range, the solution has an imaginary component (see, for example, the solution for the dimer in Ref. 33). Thus, the desire to overcome this pathological behavior, and to extend the QDO model to further improve the description of interatomic interactions, has stimulated a long list of recent theoretical and numerical developments.^{17,19–21,23,34}

A first direction to extend the QDO model beyond the dipole approximation is that of considering full Coulomb interactions between the particles^{16–18,23,34,36} of the different QDOs [Fig. 1(b)], i.e., introducing the full Coulomb QDO (CQDO) model, which is the main subject of study in this work. As we will show below, the CQDO model not only allows us to consistently capture

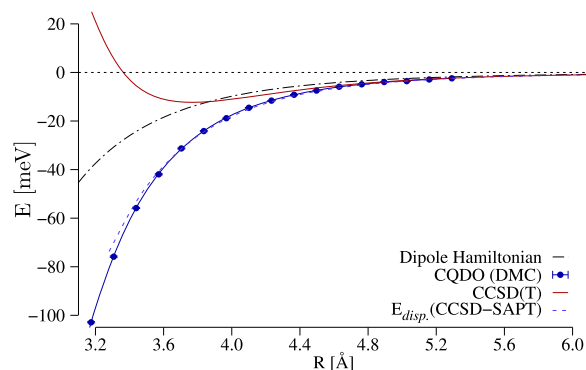


FIG. 2. Binding energy of the Argon dimer obtained with CCSD(T),³⁵ compared to the Coulomb coupled QDO (CQDO) model obtained with the DMC method (the QDO parameterization from Ref. 18) and the Mol. + J wavefunction, and to the dispersion energy ($E_{disp.}$) from SAPT-CCSD in Ref. 35. We also show the potential energy surface of the QDO model in the dipole approximation limit (QDO).³³

multipolar dispersion interactions between atoms but also introduces additional contributions at the short range due to quantum delocalization.

In Fig. 2, we demonstrate the high promise of the CQDO model for capturing the contribution of correlation energy to the binding energy of Argon dimer due to its ability to describe multipolar interactions. The reference binding energy curve is computed by the CCSD(T) method, and the contribution of correlation (or dispersion) energy to binding was calculated using the electronic symmetry-adapted perturbation theory (SAPT) based on the coupled-cluster (CCSD) wavefunction for Ar monomers. Interestingly, when solving the CQDO model for the Argon dimer (Fig. 2) using the diffusion Monte Carlo (DMC) method with the parameterization presented in Ref. 18, the dispersion energy is captured with excellent accuracy at all relevant distances compared to CCSD-SAPT.^{23,35} Achieving such accuracy with the CQDO model is a highly non-trivial result as the interactions between 16 valence electrons in Ar₂ are effectively described by just two harmonic oscillators without using any empirical information about bonding. Similarly, accurate results are obtained for other noble-gas dimers, including Ne₂, Kr₂, and Xe₂, as discussed in Ref. 23. In contrast, the dipole approximation, using the same set of parameters, tends to underestimate the binding energy of Ar₂ and other noble-gas dimers, although the dipole approximation becomes sufficiently accurate at interatomic distances beyond 4.6 Å for Ar₂ (see Fig. 2).

These results, which show the advantage of the full CQDO model in comparison to the dipole approximation, also highlight the limitations of the CQDO with a fixed parameterization, which can describe the dispersion contribution to the energy but is unable to describe the full potential-energy surface from the repulsive to the attractive regime. To achieve this challenging goal, further generalization of the CQDO model is required, and an important first step is to obtain the exact solution for all values of the interatomic distance.

In the numerous works that have attempted to tackle the generalization of the CQDO model to better reproduce the potential-energy surface (PES) of dimers or molecular clusters, the authors

have solely focused on the description of the large distance regimes, characteristic of dispersion interactions, in which the model has been shown to be efficient, without attempting to discuss the exact solution for all values of the relative distance between QDOs.^{16–18,23,34}

In particular, Full Configuration Interaction (FCI)¹⁷ has been applied to the CQDO model, however, without converging the solution to the complete basis set limit (as will be discussed and shown in Fig. 4). Quantum Monte Carlo (QMC) methods have also been applied to solve the CQDO Hamiltonian, yet employing empirical damping functions to remove the divergences arising from the Coulomb potentials, which were not treated with the correct variational wavefunction.³⁷

In this work, we construct an accurate solution of the CQDO model at all distances by proposing a general wavefunction that can be optimized using QMC methods and eventually FCI approaches (with an appropriate change of one-particle basis set). We focus, without loss of generality, on the homogeneous CQDO dimer in order to study its potential-energy surface (PES) as a function of the three parameters that characterize the QDOs, i.e., frequency, charge, and reduced mass. Through such analysis, we show that, following a similar procedure to the one proposed in Refs. 19–21, it is possible to extend the applicability of the model to describe chemical bonds beyond dispersion interactions, such as the PES of the covalent bond in the H₂ molecule.

II. COULOMB INTERACTING QUANTUM DRUDE OSCILLATORS

The first difference between the QDO model in the dipole approximation and that with full Coulomb interactions (CQDO)^{17,18,23,34} can be found in the expression of the single particle Hamiltonian in Eq. (1), namely, that for the *i*th drudon of a system of *N* QDOs assumes the more general form

$$\hat{h}_i^C(\mathbf{r}_i) = -\frac{1}{2\mu_i} \nabla_{\mathbf{r}_i}^2 + v(\mathbf{r}_i), \quad (4)$$

where the single-particle potential energy $v(\mathbf{r}_i)$ also includes the Coulomb interactions between the quantum particle and the other QDO centers,

$$v_i(\mathbf{r}_i) = \frac{1}{2} \mu_i \omega_i^2 |\mathbf{d}_i|^2 - \sum_{j \neq i}^N \frac{q_i q_j}{|\mathbf{r}_i - \mathbf{R}_j|}. \quad (5)$$

This single particle potential is different for each drudon, as shown for the QDO dimer in Fig. 3, meaning that each drudon, no matter if characterized by identical parameters (q , μ , ω), is a distinguishable particle. The full Hamiltonian of *N* QDOs interacting via full Coulomb potentials will have the following form:

$$\hat{H}^C = \sum_{i=1}^N \hat{h}_i^C(\mathbf{r}_i) + \sum_{j>i=1}^N v_{ij}(\mathbf{r}_i, \mathbf{r}_j) + v_{\text{ext}}(\bar{\mathbf{R}}), \quad (6)$$

where $v_{ij}(\mathbf{r}_i, \mathbf{r}_j) = \frac{q_i q_j}{|\mathbf{r}_i - \mathbf{r}_j|}$ is the Coulomb interaction between two drudons and $v_{\text{ext}}(\bar{\mathbf{R}}) = \sum_{j>i=1}^N \frac{q_i q_j}{|\mathbf{R}_i - \mathbf{R}_j|}$ is the constant contribution coming from the Coulomb interaction between all the QDO centers.

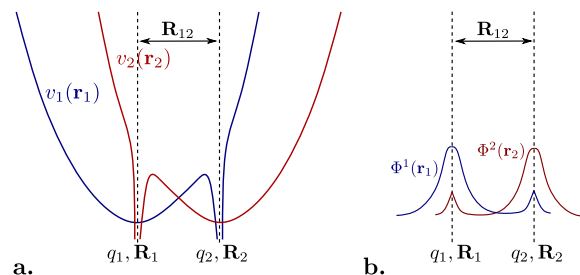


FIG. 3. (a) Schematic representations of the one body potentials $v_1(\mathbf{r}_1)$ and $v_2(\mathbf{r}_2)$ associated with each drudon for a system of two interacting CQDOs [Eq. (5)]. (b) Single particle molecular orbitals of the two drudons [Eq. (9)] as linear combinations of a Gaussian function and a Slater-type orbital.

In contrast to the dipole Hamiltonian, Eq. (6) is not exactly diagonalizable; hence, solving it requires the construction of an approximate yet robust wavefunction, which depends on the relative positions $\bar{\mathbf{R}}$ of the QDO centers, and this task will be discussed in Sec. III.

III. APPROXIMATE WAVEFUNCTION FOR THE QUANTUM DRUDE OSCILLATORS

As anticipated in the Introduction, the previous works that approached the solution of the CQDO model focused essentially on the correct description of the large distance regimes that characterize dispersion interactions.^{17,18,23,34} At these distances, the solution can be written as a perturbation of the solutions of two non-interacting QDOs, represented by isotropic Gaussian orbitals, which are deformed by additional couplings.

For this reason, in the FCI approach of Sadhukhan and Manby,¹⁷ the authors constructed a variational space of the homogeneous CQDO dimer as the linear combination of a set of single QDO excitations of the two localized oscillators, highlighting the convergence difficulties in the short-distance limit (see also Fig. 4).

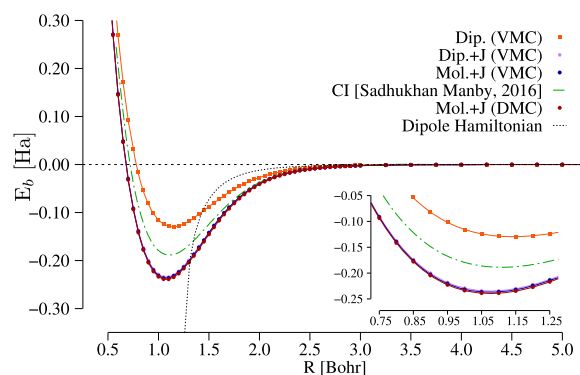


FIG. 4. Binding energy E_b for the CQDO homogeneous dimer with $\omega = \mu = q = 1$. The black dotted line represents the solution of the Hamiltonian in the limit of dipole approximation [Eq. (2)]. The CI results are taken from Ref. 17. The VMC Dip. + J PES is not clearly visible since it almost corresponds to the VMC Mol. + J one. The difference between the two at the equilibrium length is only of a few mHa.

On the other hand, in the QMC approach from Martyna and co-workers,^{18,37} the authors used a trial wavefunction built from the product of the solution of non-interacting harmonic oscillators adding a fixed three-body correlation function constructed analytically to reproduce the long-range interactions between the QDOs that are responsible for the reciprocal polarization. Yet, this wavefunction was not built to describe the cusp conditions of the true wavefunction that arise from the Coulomb interactions between particles, and therefore, damping functions were employed to remove those divergences.

Finally, a more general form was used in the work of Ditte *et al.*,²³ in which the authors proposed a variational wavefunction inspired by the exact solution of the QDO model in the dipole interaction limit [Eq. (2)],

$$\Psi^{\text{Dip}}(\bar{\mathbf{r}}) = \exp\{-\bar{\mathbf{d}}^T \mathbf{A} \bar{\mathbf{d}}\}, \quad (7)$$

where \mathbf{A} is a symmetric $3N \times 3N$ coupling matrix and $\bar{\mathbf{d}}$ is the $3N$ vector of the distances between the drudons and their corresponding centers, i.e., $\{\mathbf{d}_i = \mathbf{r}_i - \mathbf{R}_i \mid \forall i \in [1, N]\}$.^{5,23} While the diagonal elements of the parameters' matrix \mathbf{A} contain the Gaussian solutions of the isolated QDOs and upon relaxation they describe the on-site polarization of the oscillators, the off-diagonal elements represent the coupling of the various oscillators along the three dimensions. Despite the fact that for distances characteristic of the dispersion interactions this solution is a good approximation, it fails to converge to the proper state for the CQDO model for all values of the QDO positions $\bar{\mathbf{R}}$ since it does not take into account the form of the single-particle potential energies in Eq. (5).

In order to construct a more general and accurate solution to Eq. (6), here we address all the main aspects and properties that the solution should incorporate, following a similar approach to the one used for many-electron systems in the basis of molecular orbitals.^{38–40}

If we consider the i th drudon, since the quantum particle interacts with its center through a harmonic potential, it is known that the solution in this region must reflect a Gaussian-type orbital (GTO) of the type $\phi_i(\mathbf{r}_i) \propto \exp(-\frac{\mu_i \omega_i d_{ij}^2}{2})$. Yet, the same drudon will interact with all the other $N - 1$ QDO centers via a Coulomb potential, meaning that the wavefunction must satisfy the cusp conditions,⁴¹

$$\frac{1}{\langle \Psi \rangle} \frac{\partial \langle \Psi \rangle}{\partial d_{ij}} \Big|_{d_{ij}=0} = q_i q_j \mu_j \quad \forall j \neq i, \quad (8)$$

where $\langle \Psi \rangle$ represents the angular average of the wavefunction and $d_{ij} = |\mathbf{r}_i - \mathbf{R}_j|$ is the absolute distance between the i th drudon and the j th QDO center. Thus, around the j th center, the single-particle orbital of the i th drudon will have the form of an exponential function, i.e., a Slater-type orbital (STO), proportional to $\phi_j(\mathbf{r}_i) \propto \exp(-q_i q_j \mu_j d_{ij})$.

Considering these characteristics, approximate single particle orbitals should be written as a linear combination of Gaussian and Slater-type functions (see Fig. 3),

$$\Phi^i(\mathbf{r}_i) \approx \alpha_i^i e^{(-\frac{\mu_i \omega_i}{2} d_{ij}^2)} + \sum_{j \neq i}^N \alpha_j^i e^{(-q_i q_j \mu_j d_{ij})}, \quad (9)$$

where α_j^i are a set of parameters, with indices $i, j \in [1, N]$. These orbitals can be generalized following the same approach used to define electronic molecular orbitals, and thus, in this work, they are written as a linear combination

$$\Phi^i(\mathbf{r}_i) = \sum_{q=1}^Q \alpha_q^i \phi_q(\mathbf{r}_i) \quad (10)$$

of Q atomic-like orbitals $\phi_q(\mathbf{r}_i)$ constituting the basis set of the system of QDOs and are written as a linear combination of Gaussian-type orbitals (GTOs) centered on the positions of various QDOs $\bar{\mathbf{R}}$, whose linear and exponential parameters are fully optimized. In particular, in all our calculations, each QDO is represented through a (3s1s)/(1s1s) contracted basis set, where the uncontracted 1s orbital is used to describe the Gaussian solution around the quadratic potential and the contracted (3s)/(1s) orbital is used to describe the Slater solution centered on the drudon–nucleus Coulomb potential.

The use of GTOs in the place of exponential functions clearly introduces an error in the description of the one-body cusp in Eq. (8) that can be eliminated through a Jastrow factor^{42,43} that is normally used in quantum Monte Carlo trial wavefunctions of the form

$$J_1(\bar{\mathbf{r}}) = \exp\left(\sum_{i \neq j}^N q_i q_j \mu_j f_{1b}(d_{ij}; \boldsymbol{\gamma})\right), \quad (11)$$

where $f_{1b}(d_{ij}; \boldsymbol{\gamma})$ is a parametric function that only depends on the distance between two particles (in this case the i th drudon and the j th QDO center) that for $d_{ij} \rightarrow 0$ has the property of going linearly to zero, i.e., $f(d_{ij}) \approx d_{ij}$, and decays to zero as the distance increases $f(d_{ij}) \rightarrow 0$ as $d_{ij} \rightarrow \infty$.

Another property of the wavefunction will be the explicit correlation between the pairs of drudons, which is introduced through two-body Coulomb potential $v_{ij}(\mathbf{r}_i, \mathbf{r}_j)$ in Eq. (6). A first correlation function between drudonic pairs can be introduced, considering that in the limit of two overlapping drudons, the exact wavefunction has a two-body cusp of the form

$$\frac{1}{\langle \Psi \rangle} \frac{\partial \langle \Psi \rangle}{\partial r_{ij}} \Big|_{r_{ij}=0} = q_i q_j \frac{\mu_i \mu_j}{\mu_i + \mu_j} \quad \forall j \neq i. \quad (12)$$

This requisite can be satisfied again through a Jastrow factor of the type

$$J_2(\bar{\mathbf{r}}) = \exp\left(\sum_{i > j}^N q_i q_j \frac{\mu_i \mu_j}{\mu_i + \mu_j} f_{2b}(r_{ij}; \boldsymbol{\eta})\right), \quad (13)$$

where $f_{2b}(r_{ij}; \boldsymbol{\eta})$ is a parametric function with similar properties to the one defined in Eq. (11) to reproduce the one-body cusp condition.

From these considerations, by combining Eqs. (10), (11), and (13), we can write a first approximation to the explicitly correlated wavefunction as

$$\Psi_T^{\text{Mol+J}}(\bar{\mathbf{r}}) = \left[\prod_{i=1}^N \Phi^i(\mathbf{r}_i) \right] J_1(\bar{\mathbf{r}}) J_2(\bar{\mathbf{r}}), \quad (14)$$

which will be referred to as Mol. + J in Secs. IV–VI, where the one-body cusp function is written as

$$f_{1b}(d_{ij}; \boldsymbol{\gamma}) = -\frac{e^{-\gamma_0 d_{ij}}}{\gamma_0} + \sum_{m=1}^M \gamma_m e^{-\gamma_{M+m} d_{ij}^2} \quad (15)$$

and the two-body has a form inspired by Padé's approximation,⁴⁴

$$f_{2b}(r_{ij}; \boldsymbol{\eta}) = -\frac{1}{\eta_0(1 + \eta_0 r_{ij})} + \sum_{m=1}^M \eta_m e^{-\eta_{M+m} r_{ij}^2}. \quad (16)$$

In Eqs. (15) and (16), the two vectors of $2M + 1$ parameters $\boldsymbol{\gamma}$ and $\boldsymbol{\eta}$ are both optimized. In our calculations, we assume $M = 5$.

In order to assess approximate wavefunctions, two alternative trial wavefunctions will be considered in this work: (i) dipolar wavefunction in Eq. (7), referred to as Dip.; (ii) the same dipolar wavefunction enhanced with the Jastrow factors defined in Eqs. (11) and (13),

$$\Psi_T^{\text{Dip.}+J}(\bar{\mathbf{r}}) = \exp\{-\bar{\mathbf{d}}^T \mathbf{A} \bar{\mathbf{d}}\} J_1(\bar{\mathbf{r}}) J_2(\bar{\mathbf{r}}), \quad (17)$$

which will be referred to as Dip. + J.

IV. QUANTUM MONTE CARLO METHODS

To solve the general Hamiltonian in Eq. (6) over the explicitly correlated trial wavefunctions [Eqs. (7), (14), and (17)] presented in this work, the most common and efficient approach is to employ quantum Monte Carlo (QMC)^{45–47} methods, which are integration techniques based on stochastic procedures.

To recall the basic theory behind QMC, let us consider the most common of these methods, i.e., the variational Monte Carlo (VMC) method. In VMC, the integration of the energy functional $E[\Psi_T(\bar{\mathbf{x}}, \boldsymbol{\alpha})] = (\int \Psi_T^*(\bar{\mathbf{x}}, \boldsymbol{\alpha}) \hat{H} \Psi_T(\bar{\mathbf{x}}, \boldsymbol{\alpha}) d\bar{\mathbf{x}}) / (\int |\Psi_T(\bar{\mathbf{x}}, \boldsymbol{\alpha})|^2 d\bar{\mathbf{x}})$ of the Hamiltonian operator \hat{H} over a chosen trial wavefunction $\Psi_T(\bar{\mathbf{x}}, \boldsymbol{\alpha})$ is obtained by generating a set of configurations $\bar{\mathbf{x}}^{48}$ according to the probability density $\Pi(\bar{\mathbf{x}}) \propto |\Psi_T(\bar{\mathbf{x}}, \boldsymbol{\alpha})|^2$. Through this sampling, the energy functional is estimated as the statistical average of the local energy $E_l(\bar{\mathbf{x}}) = \hat{H} \Psi_T(\bar{\mathbf{x}}, \boldsymbol{\alpha}) / \Psi_T(\bar{\mathbf{x}}, \boldsymbol{\alpha})$ values computed for each configuration, $E \approx \mathbb{E}[E_l] = \frac{1}{N} \sum_{i=1}^N E_l(\bar{\mathbf{x}}_i)$, with an associated error $\sigma_E = \sqrt{\text{Var}[E_l] / N}$ that decreases as the square root of the number of samples, and is proportional to the square root of the variance $\text{Var}[E_l] = \sum_{i=1}^N (E_l(\bar{\mathbf{x}}_i) - \mathbb{E}[E_l])^2 / (N - 1)$.

Within this framework, we optimize the full set of variational parameters $\boldsymbol{\alpha}$ through the stochastic reconfiguration energy minimization procedure introduced by Sorella in Ref. 49.

Moreover, since our systems are comprised of distinguishable particles, the exact wavefunction will be strictly positive, and thus, we can efficiently apply projection techniques, such as diffusion Monte Carlo (DMC),^{45–47} to go beyond the limits of the optimized variational trial wavefunctions $\Psi_T(\bar{\mathbf{x}}, \boldsymbol{\alpha})$, converging to the correct value of the total energy. Here, we will apply the DMC algorithm with importance-sampling guided by the already excellent approximations $\Psi_T(\bar{\mathbf{x}}, \boldsymbol{\alpha})$ to the ground state. The time step used in all the calculations is of 0.001 au.

All calculations presented in this work are done with the QMeCha⁵⁰ QMC package, published in a private Github repository.

V. THE HOMOGENEOUS CQDO DIMER

Before analyzing the variation of the CQDO model's properties with respect to the frequency ω , the mass μ , and the charge q varied independently with respect to the reference case $\mu = q = \omega = 1$, we must study the convergence of the variational wavefunctions, Dip., Dip. + J., and Mol. + J., constructing the PESs at VMC and DMC levels for the homogeneous CQDO dimer ($\mu = q = \omega = 1$).

From the results displayed in Fig. 4, we can see how the Dip. wavefunction is unable to properly reproduce the binding energy profile in the short range since it cannot describe the tunneling effects of the drudon from its center toward the attractive Coulomb potential on the opposite QDO. The introduction of the Jastrow factor in the Dip. + J. wavefunction greatly improves the variational results since it is able to take into account both the correlation of the drudon around the attractive Coulomb potential and the two-body correlation of the two drudons that become important as the two QDOs come together. In fact, at the VMC level, the latter wavefunction recovers more than 0.10 Ha in the binding energy with respect to the former. Finally, a small improvement, of about 2 mHa at the equilibrium distance, with respect to the Dip. + J. wavefunction can be obtained with the Mol. + J., since the single-particle orbitals also account for the tunneling effects of the drudons in the short range. Moreover, the VMC PES obtained with the Mol. + J. trial wavefunction is nearly identical to the converged DMC energy obtained with the same wavefunction, with a difference of about 2.3 mHa at the equilibrium distance. As discussed in Sec. II, since the system is built from distinguishable particles, DMC will always converge to the exact solution no matter the trial wavefunction employed.

Taking this into account, in Fig. 4, we also compare our results with the full CI PES, previously reported in Ref. 17 for the same system. As previously anticipated, it is clear that due to restricted configuration space, the CI calculations were not properly converged toward the exact solution obtained with DMC, reporting a maximum discrepancy with our results of more than 0.05 Ha, i.e., about 20% error.

Considering these initial results, we will employ the Mol. + J. trial wavefunction as the guiding function for the DMC calculations used to study the behavior of the CQDO model in the limit of full convergence.

VI. PARAMETERIZATION OF THE CQDO MODEL

To better understand the behavior of the CQDO model in describing atomic interactions, let us first study how the changes in the three parameters μ , q , and ω affect the potential energy surface of two interacting QDOs.

In Fig. 5, starting from the CQDO model with $\mu = q = \omega = 1$, in each panel, we report the change in the PES obtained by varying one by one the three parameters in a range between [0.25, 1.50], while keeping the rest of them fixed.

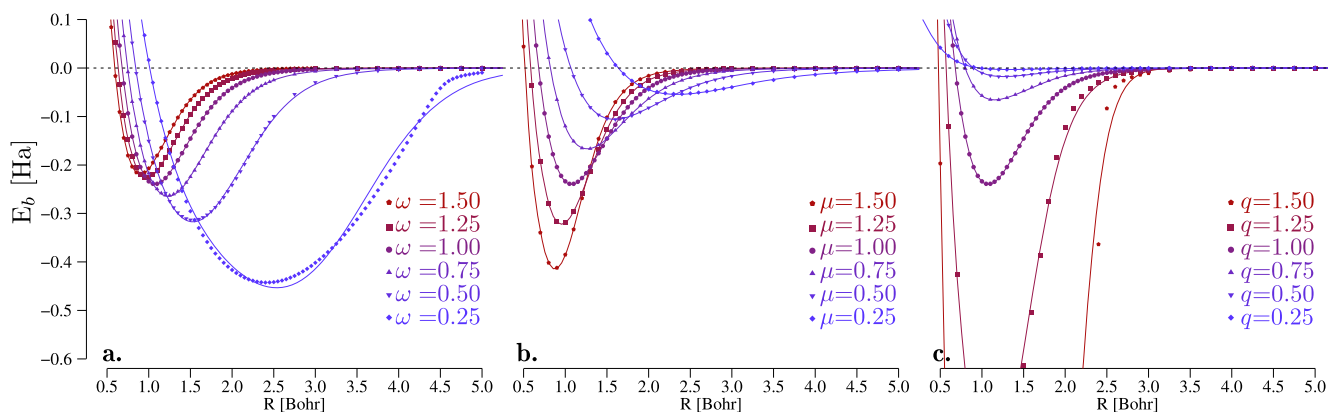


FIG. 5. DMC binding energies E_b for the CQDO homogeneous dimer obtained with the Mol. + J wavefunction [Eq. (14)]: (a) $\mu = q = 1$ and variable $\omega \in [0.25, 1.50]$. (b) $\omega = q = 1$ and variable $\mu \in [0.25, 1.50]$. (c) $\omega = \mu = 1$ and variable $q \in [0.25, 1.50]$. All the curves are interpolated with the ELJ function described in Eq. (18).

Each PES is interpolated using the Extended Lennard-Jones (EL) potential,⁵¹ which is reported to be the most accurate in reproducing various types of chemical interactions.⁵² The ELJ potential has a functional form of the type

$$E(R) = D_e \left[1 - \left(\frac{R_e}{R} \right)^{n(R)} \right]^2, \quad (18)$$

where

$$n(R) = \beta_0 + \beta_1 \zeta + \beta_2 \zeta^2 + \beta_3 \zeta^3 \quad (19)$$

with $\zeta = \frac{R-R_e}{z^4 R + R_e}$, where $z = \frac{R-R_e}{R+R_e}$ and $q = 2$. The interpolations are obtained optimizing all the six parameters D_e , R_e , β_0 , β_1 , β_2 , and β_3 . From the results in Fig. 5, it is clear that the ELJ potential overall interpolates very well the PESs at all distances, except for those obtained with low frequency or high charge, which correspond to a strong delocalization of the drudonic particles.

As a matter of fact, since the frequency is directly connected to the localization of the particles on their center, as it diminishes, the drudons become progressively delocalized with the consequent lowering of the binding energy and elongation of the equilibrium “bond” length [Fig. 5(a)].

On the other hand, μ affects both the quadratic potential and the kinetic energy of the particles of the system. In fact, the lowering of the mass of the drudons has the effect of increasing their kinetic energy and lowering the quadratic barrier, thus increasing polarizability [Fig. 5(b)]. Yet, the quadratic potential quadratically depends on the frequency ω and only linearly on μ ; thus, the barrier changes more slowly, and thus, the reduction of the mass, although increasing the polarizability in the long-range, does not induce a strong delocalization of the drudon on the other center.

Clearly, the delocalization effect that is observed with the decrease of the frequency is also stimulated by the increase of the charge q that regulates the Coulomb attraction between the

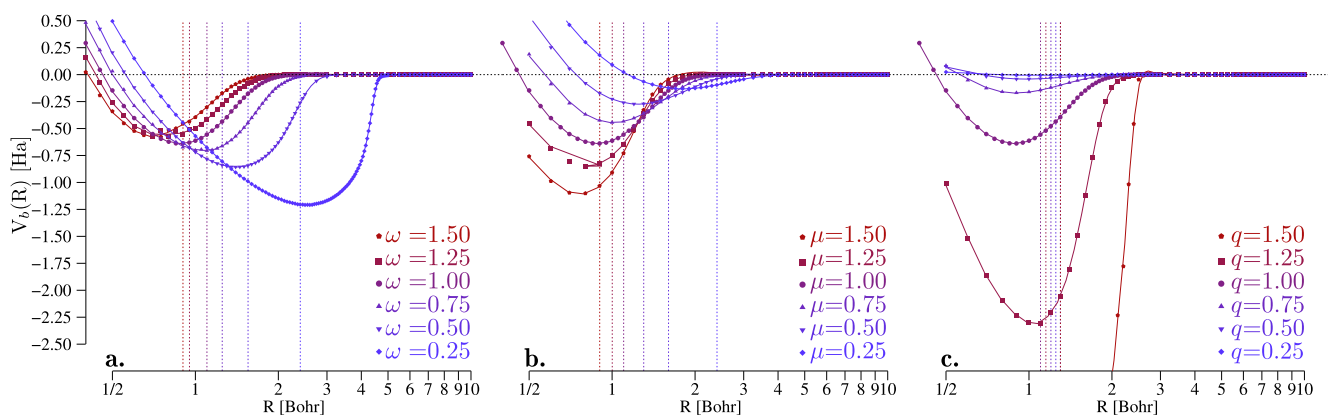


FIG. 6. Potential energy of the CQDO model shifted of its value in the dissociation limit $V_b(R) = V(R) - \frac{3}{2}\omega$ obtained with DMC. As for Fig. 5, (a) $\mu = q = 1$ and variable $\omega \in [0.25, 1.50]$; (b) $\omega = q = 1$ and variable $\mu \in [0.25, 1.50]$; and (c) $\omega = \mu = 1$ and variable $q \in [0.25, 1.50]$. The vertical lines correspond to the equilibrium lengths of the PES in Fig. 5.

drudonic particles and the opposite centers [Fig. 5(c)]. This effect is less visible in the long-range regime, for which the QDOs act as effectively neutral systems,^{18,21,23} but it becomes important in the short range for which the quadratic barrier that localizes the QDOs becomes weaker, enabling the drudons to drift toward the opposite center.

The fact that in the long-range regime the QDOs act as neutral systems can simply be observed by plotting the potential energy of the CQDO minus the dissociation value, i.e., $\frac{3}{2}\omega$ (Fig. 6). This value is always very small at distances around 4–5 bohr, meaning that in those ranges, the interaction between the two QDOs originates from dispersion contributions.

By analyzing these results, it becomes possible to choose the set of parameters ω , μ , and q to reproduce PESs of chemical bonds, beyond dispersion interactions. This can be, for example, achieved by defining a set of parameters that are dependent on the relative distances between the QDO centers (or by changing the effective inter-QDO potential).

If we consider the simplest case of the H₂ molecule, it is possible to reproduce its PES by varying the frequency ω of the QDO model as a function of the distance (Fig. 7). As a matter of fact, by varying the frequency ($\mu = q = 1$), we can obtain a set of CQDO PESs each intersecting the H₂ PES at various values of the distance R , i.e., $E[\text{H}_2(R)] + 2E[\text{H}] = E[\text{CQDO}_2(\omega; R)] - 2E[\text{CQDO}(\omega)]$, which corresponds to setting $E[\text{H}_2(R)] - E[\text{CQDO}_2(\omega; R)] + 1 + 3\omega = 0 \forall R$.

By plotting the values of the frequencies ω for which the corresponding QDO curves intersect the H₂ PES, as a function of the interatomic distance R , we obtain the data displayed in Fig. 7(a).

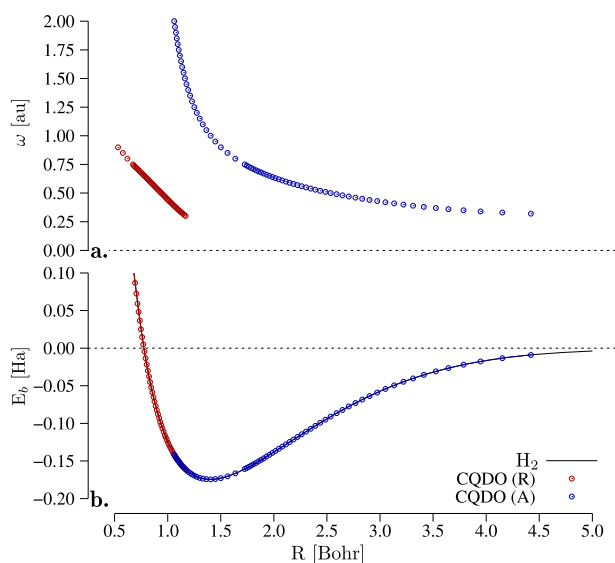


FIG. 7. (a) ω as a function of the position R for which the corresponding CQDO(ω) curves intersect the PES of the H₂ molecule. For a small distance of ≈ 1 bohr, we observe that the CQDO(ω) curves intersect the PES of H₂ in two points. (b) CQDO(ω ; R) PES (red and blue circles) obtained by varying the frequency according to the values in (a), compared with the PES of H₂ (black line) obtained with accurate DMC results.

By selecting for each R the values of ω to match the H₂ PES, we obtain the binding profile shown in Fig. 7(b).

Here, we must remark that these are only a set of preliminary tests where only the frequency of the QDO model was changed to reproduce a given binding energy curve for a chemically bonded system. Yet, we hypothesize that matching the response properties (polarizability and dispersion coefficients) for QDO and electronic systems for different values of R might lead to a more promising QDO model for chemical bonding. In addition, a QDO model for all relevant interatomic distances might need to be based on a more general effective single-particle potential. We defer the assessment of these promising directions to future work.

VII. CONCLUSIONS AND OUTLOOK

The coupled QDO model has been successfully applied to describe dispersion interactions in molecules and materials, being at the basis of modern vdW approaches,^{10,11} such as the many-body dispersion method.¹⁵ To describe these long-range interactions, the QDO model is usually applied in the dipole approximation, given that the Hamiltonian can be diagonalized without introducing a significant computational overhead in electronic-structure calculations.^{32,53}

Thus far, the focus of the coupled QDO model has primarily been on capturing long-range interactions.^{19,21,34,54} However, in the short-range regime, the bare dipole-coupled QDO model has imaginary solutions, and in general, it is unable to explicitly describe correlations arising from the higher multipolar moments of the charge distribution.

These limitations can be partially overcome through the use of the Coulomb-coupled QDO model, for which we presented an accurate solution without loss of generality for the case of the homogeneous CQDO dimer.

The construction of this solution stands as an important milestone since it presents a variational framework to pursue a more general parameterization of the drudonic model to reproduce a wider set of chemical interactions, beyond those governed by long-range electron correlation. As shown in this work, for the case of the H₂ molecule, this can be achieved, for example, by introducing an explicit dependence of the QDO parameterization on the relative distances between the oscillation centers.

Among many possible directions, our future work will explore a broader set of chemically bonded systems, different ways to parameterize one-particle and two-particle potentials in the CQDO model, the transition regime between bonded and non-bonded interactions, going beyond atomic dimers, and developing an efficient parameterization of the variational wavefunctions for Coulomb-coupled QDOs.

ACKNOWLEDGMENTS

M.D. and M.B. thank Jorge Alfonso Charry Martinez for participating in the development of the QMeCha code. AT acknowledges the financial support from ERC-2021-ADG-FITMOL (ID:101054629). M.B. acknowledges financial support from the Luxembourg National Research Fund (Grant No. INTER/DFG/18/12944860). The calculations presented in this paper

were carried out using the HPC facilities of the University of Luxembourg⁵⁵ (see hpc.uni.lu). An award of computer time was provided by the Innovative and Novel Computational Impact on Theory and Experiment (INCITE) program. This research used resources of the Argonne Leadership Computing Facility, which is a DOE Office of Science User Facility supported under Contract No. DE-AC02-06CH11357.

AUTHOR DECLARATIONS

Conflict of Interest

The authors have no conflicts to disclose.

Author Contributions

Matej Ditte: Data curation (equal); Formal analysis (equal); Investigation (equal); Methodology (equal); Software (equal); Writing – original draft (equal); Writing – review & editing (equal). **Matteo Barborini:** Data curation (equal); Formal analysis (equal); Investigation (equal); Methodology (equal); Software (equal); Visualization (equal); Writing – original draft (equal); Writing – review & editing (equal). **Alexandre Tkatchenko:** Formal analysis (equal); Funding acquisition (lead); Investigation (equal); Project administration (lead); Resources (lead); Supervision (lead); Validation (lead); Writing – original draft (equal); Writing – review & editing (equal).

DATA AVAILABILITY

The data that support the findings of this study are available from the corresponding author upon reasonable request.

REFERENCES

- 1 F. London, “The general theory of molecular forces,” *Trans. Faraday Soc.* **33**, 8b–26b (1937).
- 2 P. Drude, “Zur elektronentheorie der metalle,” *Ann. Phys.* **306**, 566–613 (1900).
- 3 P. Drude, *The Theory of Optics* (Dover Publications, New York, 1959), pp. 382–417.
- 4 J. O. Hirschfelder, C. F. Curtiss, and R. B. Bird, *The Molecular Theory of Gases and Liquids* (John Wiley & Sons, New York, 1954), pp. 956–960, 877–890.
- 5 W. L. Bade, “Drude-model calculation of dispersion forces. I. General theory,” *J. Chem. Phys.* **27**, 1280–1284 (1957).
- 6 F. Wang and K. D. Jordan, “A Drude-model approach to dispersion interactions in dipole-bound anions,” *J. Chem. Phys.* **114**, 10717–10724 (2001).
- 7 T. Sommerfeld and K. D. Jordan, “Quantum Drude oscillator model for describing the interaction of excess electrons with water clusters: An application to (H₂O)₁₃-,” *J. Phys. Chem. A* **109**, 11531–11538 (2005).
- 8 G. Lamoureux and B. Roux, “Modeling induced polarization with classical Drude oscillators: Theory and molecular dynamics simulation algorithm,” *J. Chem. Phys.* **119**, 3025–3039 (2003).
- 9 J. A. Crosse and S. Scheel, “Atomic multipole relaxation rates near surfaces,” *Phys. Rev. A* **79**, 062902 (2009).
- 10 J. A. Lemkul, J. Huang, B. Roux, and A. D. J. MacKerell, “An empirical polarizable force field based on the classical Drude oscillator model: Development history and recent applications,” *Chem. Rev.* **116**, 4983–5013 (2016).
- 11 J. Hermann, R. A. DiStasio, and A. Tkatchenko, “First-principles models for van der Waals interactions in molecules and materials: Concepts, theory, and applications,” *Chem. Rev.* **117**, 4714–4758 (2017).

¹²T. Odbadrakh, V. Voora, and K. Jordan, “Application of electronic structure methods to coupled Drude oscillators,” *Chem. Phys. Lett.* **630**, 76–79 (2015).

¹³T. T. Odbadrakh and K. D. Jordan, “Dispersion dipoles for coupled Drude oscillators,” *J. Chem. Phys.* **144**, 034111 (2016).

¹⁴K. R. Bryenton and E. R. Johnson, “Many-body dispersion in model systems and the sensitivity of self-consistent screening,” *J. Chem. Phys.* **158**, 204110 (2023).

¹⁵A. Tkatchenko, R. A. DiStasio, R. Car, and M. Scheffler, “Accurate and efficient method for many-body van der Waals interactions,” *Phys. Rev. Lett.* **108**, 236402 (2012).

¹⁶M. Stöhr, M. Sadhukhan, Y. Al-Hamdani, J. Hermann, and A. Tkatchenko, “Coulomb interactions between dipolar quantum fluctuations in van der Waals bound molecules and materials,” *Nat. Commun.* **12**, 137 (2021).

¹⁷M. Sadhukhan and F. R. Manby, “Quantum mechanics of Drude oscillators with full Coulomb interaction,” *Phys. Rev. B* **94**, 115106 (2016).

¹⁸A. P. Jones, J. Crain, V. P. Sokhan, T. W. Whitfield, and G. J. Martyna, “Quantum Drude oscillator model of atoms and molecules: Many-body polarization and dispersion interactions for atomistic simulation,” *Phys. Rev. B* **87**, 144103 (2013).

¹⁹D. V. Fedorov, M. Sadhukhan, M. Stöhr, and A. Tkatchenko, “Quantum-mechanical relation between atomic dipole polarizability and the van der Waals radius,” *Phys. Rev. Lett.* **121**, 183401 (2018).

²⁰O. Vaccarelli, D. V. Fedorov, M. Stöhr, and A. Tkatchenko, “Quantum-mechanical force balance between multipolar dispersion and pauli repulsion in atomic van der Waals dimers,” *Phys. Rev. Res.* **3**, 033181 (2021).

²¹S. Göger, A. Khabibrakhmanov, O. Vaccarelli, D. V. Fedorov, and A. Tkatchenko, “Optimized quantum Drude oscillators for atomic and molecular response properties,” *J. Phys. Chem. Lett.* **14**, 6217–6223 (2023).

²²A. Ambrosetti, P. Umari, P. L. Silvestrelli, J. Elliott, and A. Tkatchenko, “Optical van-der-Waals forces in molecules: From electronic bethe-salpeter calculations to the many-body dispersion model,” *Nat. Commun.* **13**, 813 (2022).

²³M. Ditte, M. Barborini, L. M. Sandonas, and A. Tkatchenko, “Molecules in environments: Toward systematic quantum embedding of electrons and Drude oscillators,” *Phys. Rev. Lett.* **131**, 228001 (2023).

²⁴A. Khabibrakhmanov, D. V. Fedorov, and A. Tkatchenko, “Universal pairwise interatomic van der Waals potentials based on quantum Drude oscillators,” *J. Chem. Theory Comput.* **19**, 7895–7907 (2023).

²⁵R. Eisenschitz and F. London, “Über das Verhältnis der van der Waalschen Kräfte zu den homöopolaren Bindungskräften,” *Z. Phys.* **60**, 491–527 (1930).

²⁶W. L. Bade and J. G. Kirkwood, “Drude-model calculation of dispersion forces. II. The linear lattice,” *J. Chem. Phys.* **27**, 1284–1288 (1957).

²⁷W. L. Bade, “Drude-model calculation of dispersion forces. III. The fourth-order contribution,” *J. Chem. Phys.* **28**, 282–284 (1958).

²⁸D. J. Margoliash and W. J. Meath, “Pseudospectral dipole oscillator strength distributions and some related two body interaction coefficients for H, He, Li, N, O, H₂, N₂, O₂, No, N₂O, H₂O, NH₃, and CH₄,” *J. Chem. Phys.* **68**, 1426–1431 (1978).

²⁹A. Tkatchenko and M. Scheffler, “Accurate molecular van der Waals interactions from ground-state electron density and free-atom reference data,” *Phys. Rev. Lett.* **102**, 073005 (2009).

³⁰A. A. Lucas, “Effect of many-body van der Waals forces on the lattice dynamics of rare-gas crystals,” *Phys. Rev.* **176**, 1093–1097 (1968).

³¹A. Dodin and P. L. Geissler, “Symmetrized Drude oscillator force fields improve numerical performance of polarizable molecular dynamics,” *J. Chem. Theory Comput.* **19**, 2906–2917 (2023).

³²A. Ambrosetti, A. M. Reilly, R. A. DiStasio, and A. Tkatchenko, “Long-range correlation energy calculated from coupled atomic response functions,” *J. Chem. Phys.* **140**, 18A508 (2014).

³³The exact solution of the QDO dimer in the dipole interaction limit that is described in Refs. 1 and 4 is of the form $E_{\pm}(R)$

$$= \frac{e_0}{2} \left(2\sqrt{1 \pm \frac{q^2}{\mu\omega^2 R^3}} + \sqrt{1 \mp 2\frac{q^2}{\mu\omega^2 R^3}} \right) \text{ and } E_0(R) = E_+(R) + E_-(R), \text{ with } \hbar = 1.$$

³⁴F. S. Cipcigan, J. Crain, V. P. Sokhan, and G. J. Martyna, “Electronic coarse graining: Predictive atomistic modeling of condensed matter,” *Rev. Mod. Phys.* **91**, 025003 (2019).

- ³⁵L. Shirkov and V. Sladek, "Benchmark CCSD-SAPT study of rare gas dimers with comparison to MP-SAPT and DFT-SAPT," *J. Chem. Phys.* **147**, 174103 (2017).
- ³⁶P. Bandyopadhyay and M. Sadhukhan, "Modeling coarse-grained van der Waals interactions using dipole-coupled anisotropic quantum Drude oscillators," *J. Comput. Chem.* **44**, 1164–1173 (2023).
- ³⁷A. Jones, A. Thompson, J. Crain, M. H. Müser, and G. J. Martyna, "Norm-conserving diffusion Monte Carlo method and diagrammatic expansion of interacting Drude oscillators: Application to solid xenon," *Phys. Rev. B* **79**, 144119 (2009).
- ³⁸W. Heitler and F. London, "Wechselwirkung neutraler Atome und homöopolare Bindung nach der Quantenmechanik," *Z. Phys.* **44**, 455–472 (1927).
- ³⁹J. C. Slater, "The theory of complex spectra," *Phys. Rev.* **34**, 1293–1322 (1929).
- ⁴⁰S. F. Boys, "Electronic wave functions - I. A general method of calculation for the stationary states of any molecular system," *Proc. R. Soc. A* **200**, 542–554 (1950).
- ⁴¹T. Kato, "On the eigenfunctions of many-particle systems in quantum mechanics," *Commun. Pure Appl. Math.* **10**, 151–177 (1957).
- ⁴²R. Jastrow, "Many-body problem with strong forces," *Phys. Rev.* **98**, 1479–1484 (1955).
- ⁴³N. D. Drummond, M. D. Towler, and R. J. Needs, "Jastrow correlation factor for atoms, molecules, and solids," *Phys. Rev. B* **70**, 235119 (2004).
- ⁴⁴H. Padé, "Sur la représentation approchée d'une fonction par des fractions rationnelles," *Ann. Sci. Éc. Norm. Supér.* **9**, 3–93 (1892).
- ⁴⁵W. M. C. Foulkes, L. Mitas, R. J. Needs, and G. Rajagopal, "Quantum Monte Carlo simulations of solids," *Rev. Mod. Phys.* **73**, 33–83 (2001).
- ⁴⁶M. H. Kalos and P. A. Whitlock, "Quantum Monte Carlo," in *Monte Carlo Methods* (John Wiley & Sons, Ltd, 2008), pp. 159–178, Chap. 8.
- ⁴⁷F. Becca and S. Sorella, *Quantum Monte Carlo Approaches for Correlated Systems* (Cambridge University Press, 2017).
- ⁴⁸N. Metropolis, A. W. Rosenbluth, M. N. Rosenbluth, A. H. Teller, and E. Teller, "Equation of state calculations by fast computing machines," *J. Chem. Phys.* **21**, 1087–1092 (1953).
- ⁴⁹S. Sorella, "Generalized lanczos algorithm for variational quantum Monte Carlo," *Phys. Rev. B* **64**, 024512 (2001).
- ⁵⁰M. Barborini, Quantum Mecha (QMeCha) package (private repository August 2023).
- ⁵¹P. G. Hajigeorgiou, "An extended Lennard-Jones potential energy function for diatomic molecules: Application to ground electronic states," *J. Mol. Spectrosc.* **263**, 101–110 (2010).
- ⁵²J. P. Araújo and M. Y. Ballester, "A comparative review of 50 analytical representation of potential energy interaction for diatomic systems: 100 years of history," *Int. J. Quantum Chem.* **121**, e26808 (2021).
- ⁵³A. J. A. Price, K. R. Bryenton, and E. R. Johnson, "Requirements for an accurate dispersion-corrected density functional," *J. Chem. Phys.* **154**, 230902 (2021).
- ⁵⁴A. Ambrosetti, D. Alfè, R. A. J. DiStasio, and A. Tkatchenko, "Hard numbers for large molecules: Toward exact energetics for supramolecular systems," *J. Phys. Chem. Lett.* **5**, 849–855 (2014).
- ⁵⁵S. Varrette, P. Bouvry, H. Cartiaux, and F. Georgatos, "Management of an academic HPC cluster: The UI experience," in *Proceedings of the 2014 International Conference on High Performance Computing & Simulation (HPCS 2014)* (IEEE, Bologna, Italy, 2014), pp. 959–967.